

# Constrained Photophysics of 5,7-dimethoxy-2,3,4,9-tetrahydro-1H-carbazol-1-one in the Bioenvironment of Serum Albumins: A Spectroscopic Endeavour Supported by Molecular Docking Analysis

Amrit Krishna Mitra<sup>1</sup> · Abhishek Sau<sup>2</sup> · Uttam Pal<sup>2</sup> · Chandan Saha<sup>3</sup> · Samita Basu<sup>2</sup>

Received: 12 January 2017 / Accepted: 4 April 2017 / Published online: 22 April 2017  
© Springer Science+Business Media New York 2017

**Abstract** This paper vividly indicates that steady state as well as time-resolved fluorescence techniques can serve as highly sensitive monitors to explore the interactions of 5,7-dimethoxy-2,3,4,9-tetrahydro-1H-carbazol-1-one with model transport proteins, bovine serum albumin (BSA) and human serum albumin (HSA). Besides these, we have used fluorescence anisotropy study to assess the degree of restrictions imparted by the micro-environments of serum albumins. Again, to speculate the triplet excited state interaction between such fluorophore and albumin proteins (BSA& HSA), laser flash-photolysis experiments have been carried out. Molecular docking experiments have also been performed to support the conclusions obtained from steady state experiments.

**Keywords** Keto-tetrahydrocarbazole · Serum albumin · Laser flash photolysis · Molecular docking · Fluorescence anisotropy

## Introduction

Serum albumins, widely studied transport proteins are abundantly found in blood plasma [1–12]. Besides being an attractive macromolecular carrier, serum albumins play a vital role

by increasing the solubility of hydrophobic drugs in the blood plasma, binding with bio-active molecules and maintaining colloid blood pressure [3, 4]. Structural facets and assets of bovine serum albumin (BSA) and human serum albumin (HSA) have been widely studied [5–27]. These two serum proteins are often used as models for several biophysical and biochemical studies as well as in diverse studies of protein chemistry [28–39]. In spite of having different folding natures, known from their structural studies, somehow sufficient resemblance in their activity is observed. Following the studies of He and Carter, BSA (583 aa) and HSA (585 aa) are characterized by a high homology in the sequence (80%) and similar conformations [34]. Molecular weights of the two proteins are also similar being 66 kDa for BSA and 66.5 kDa for HSA. According to Peters, 17 disulfide bridges and a series of nine loops, assembled in three domains (I, II, and III) each formed by two subdomains, A and B, are the fundamental constituents of such albumin proteins [39]. The principal binding sites are subdomain IIA and IIIA and they are hydrophobic in nature. Literature reviews indicate that the three-dimensional structure of human serum albumin (HSA) is believed to be resolved but for BSA, there are conflicting reports with respect to its structural aspect due to unavailability of suitable crystals for X-ray diffraction (XRD) studies. Crystallographic structure of HSA indicates that in this protein, the single tryptophan residue (Trp-214) is located in IIA binding site, while Lys-199 and His-242 are involved in the protein ligand interaction. Two tryptophan residues, Trp-212 and Trp-134 are present in BSA. Of these two tryptophan residues, Trp-212 is located in a similar hydrophobic micro-environment as the single Trp-214 in HSA (subdomain IIA), whereas Trp-134 is more solvent exposed and is localized in subdomain IA. Primary structure of BSA reveals that the subdomains contain different types of tyrosine residues; among them, Tyr-263 is located in subdomain IIA.

✉ Samita Basu  
samita.basu@saha.ac.in

<sup>1</sup> Department of Chemistry, Government General Degree College, Singur, Hooghly, West Bengal Pin:712409, India

<sup>2</sup> Chemical Sciences Division, Saha Institute of Nuclear Physics, Kolkata 700064, India

<sup>3</sup> Department of Clinical and Experimental Pharmacology, School of Tropical Medicine, Kolkata 700073, India

Detailed perusal of the protein chemistry signifies that proteins can easily adopt many conformations, ranging from more compact to a more relaxed form. Such a change in the conformations of a protein is of great interest in biophysics and structural biology as it is capable of changing linear polypeptide chains into three dimensional structures. As the unfolding of a protein progresses, new facts about the equilibrium folding states may be known [40–42]. Ionization of the side chains are the outcome of protein denaturation by pH whereas small molecules or ions, such as urea and guanidium ions, affect both the side chains and backbone hydrogen bonds [43–46]. The behaviour of denatured protein is different from that of native protein as the chemical-induced denatured protein is much exposed to water. Hence its interaction with different ligands may throw light on the structure and properties of denatured protein.

Fluorescence-probe spectroscopy of proteins is one of the most potent methodologies generating structural and dynamical information concerning the fluorophore environment [21, 47, 48]. As many bioactive small molecules bind reversibly to serum albumins, it is important to study the interactions of drugs with this protein as these studies can provide information about the structural features that determine the therapeutic effect of drugs and have become an interesting research field in life science, chemistry and clinical medicine. The study regarding the mode of binding of various molecules to serum albumins is chiefly accountable for the understanding of metabolism, bio-distribution, elimination or pharmacological effects of the drugs in the body [5–12, 14–26]. Knowledge of interaction mechanisms between endogenous and exogenous molecules and plasma proteins has a great value for researchers to understand the pharmacodynamics and pharmacokinetics of a drug candidate. The lack of toxicity and immunogenicity make it an ideal candidate for drug delivery [13–15]. Hence, knowledge of binding with serum albumins is essential [16–27].

In the present study, we have used a keto-tetrahydrocarbazole based dye, KTHC-57 (5,7-dimethoxy-2,3,4,9-tetrahydro-1H-carbazol-1-one), as the fluorescent probe (Scheme 1). The dye has been used extensively for various photophysical applications as described elsewhere [49]. In scientific literature, there is no scarcity of examples of various fluorophore-BSA/HSA binding

interactions [11–28]. However, no other research group has ever thought of investigating such an important class (keto-tetrahydrocarbazole based) of fluorophores with serum albumins. Keto-tetrahydrocarbazole skeleton is an immediate synthetic precursor of biologically active carbazole framework (corresponding carbazole derivative of KTHC-57 is given in Scheme 1). Synthesis of KTHC-57 leads to the presumption that the molecule should possess biological activity to some extent. Fundamental spectroscopic as well as photophysical study of KTHC-57 in various homogeneous and microheterogeneous media has already been performed and sufficient evidences have been acquired to designate KTHC-57 as a fluorosensor of its immediate micro-environment.

We have intended, in this present spectroscopic study on KTHC-57, to explore the potential usefulness of its fluorescence properties for understanding its interaction with relevant biological target such as proteins.

## Experimental Section

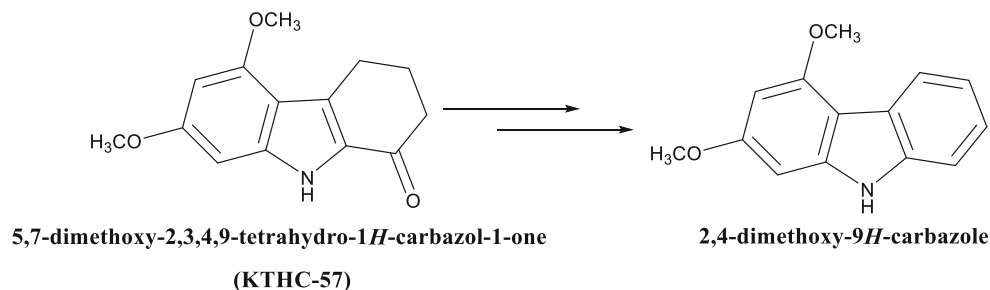
### Materials

Our fluorophore of interest KTHC-57 has been synthesized and purified following a literature procedure and is described elsewhere [49]. Phosphate buffer solution (pH ~ 7 and ionic strength = 0.15 M) has been used as the buffer solution. Bovine serum albumin (BSA) and Human serum albumin (HSA) have been purchased from Sisco Research Laboratories Pvt. Ltd. (SRL) India and used as received. Analytical grade urea from SRL, India has been used after recrystallizing twice from MeOH (AR grade, Spectrochem, India). Triple distilled water has been used for the preparation of all solutions. The solvent appeared visually transparent and its purity is also tested by running the fluorescence spectra in the studied wavelength range.

### Instrumentations and Methods

Jasco V-650 spectrophotometer and Horiba Jobin-Yvon Fluoromax-3 have been used for absorbance and fluorescence

**Scheme 1** Representative structure of 5,7-dimethoxy-2,3,4,9-tetrahydro-1H-carbazol-1-one (KTHC-57) and corresponding carbazole derivative of KTHC-57 (2,4-dimethoxy-9H-carbazole)



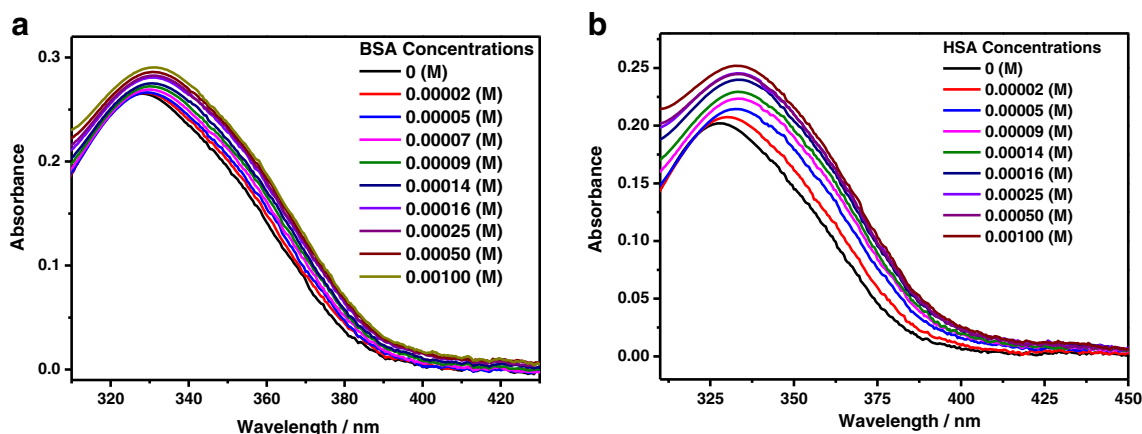


**Fig. 1** Absorption spectra of KTHC-57 with increasing concentration of (a) BSA and (b) HSA. Concentration of the compound is  $1 \times 10^{-6}$  M

measurements respectively. In all measurements, the sample concentration has been maintained in the range of  $\sim 10^{-6}$  M in order to avoid aggregation and reabsorption effects. Experiments have been carried out at an ambient temperature of 25 °C, unless otherwise specified. Only freshly prepared air-equilibrated solutions have been used for spectroscopic measurements. For spectral background corrections, a similar set of solutions in increasing BSA concentration has been prepared. During protein denaturation study by urea, spectral background corrections have been ensured with a set of solutions without a probe but containing the protein BSA (30  $\mu$ M) and respective concentrations of urea as required in each set of solutions under experiment.

Steady-state anisotropy measurements have been carried out using a Horiba Jobin-Yvon Fluoromax-4 spectrofluorimeter. The steady-state anisotropy is defined as

$$r = (IVV - G.IVH) / (IVV + 2G.IVH) \tag{1}$$

$$G = IHV / IHH \tag{2}$$

in which  $I_{VV}$  and  $I_{VH}$  are the emission intensities when the excitation polarizer is vertically oriented and the emission polarizer is oriented vertically and horizontally, respectively.  $G$  is the correction factor. Fluorescence lifetimes have been measured using a time-correlated single-photon-counting (TCSPC) spectrophotometer (Horiba Jobin-Yvon Single Photon Counting Controller Fluorohub). The sample has been excited at 340 nm using an LED to trigger the fluorescence of KTHC-57, and the signals have been collected at a magic angle of 54.7°. The lifetime is obtained using deconvolution technique which is based on a convolution integral. We have used IBH DAS 6.2 data analysis software in which reduced  $\chi^2$  and weighted residuals serve as parameters for goodness of fit. Nanosecond flash photolysis set-up (Applied Photophysics) containing Nd:YAG (Lab series, Model Lab 150, Spectra Physics) laser has been used for the measurement of transient absorption spectra. The sample has been excited at 355 nm (FWHM = 8 ns) using Nd-YAG laser (Lab series, Model Lab 150, Spectra Physics). Transient species in solution have been monitored through absorption of light from a pulsed xenon lamp (150 W) at right angle to the laser beam. The wavelength

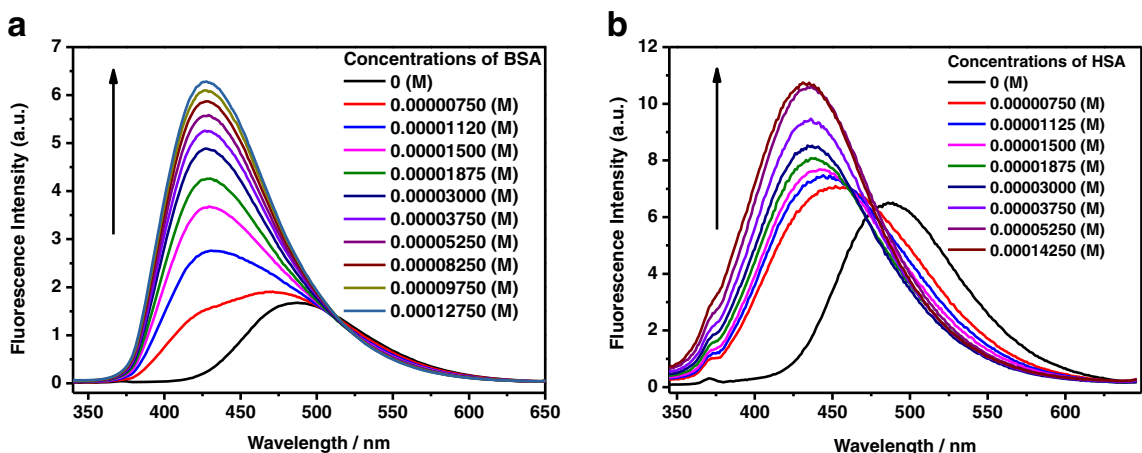


**Fig. 2** Fluorescence emission spectra of KTHC-57 in presence of different concentrations of (a) BSA and (b) HSA. Emission spectra have been taken exciting the samples at their corresponding absorption maxima

from the probe beam is dispersed with a monochromator and detected with R928 photomultiplier detector. The photomultiplier output is fed into a 600 MHz, 4 Gs/s, DSO8064A Agilent Infiniium oscilloscope and the data are transferred to Laser software running in an Iyonix range of ARM-based RISC OS computer. The samples are de-aerated for 20 min by passing pure argon gas prior to each experiment. All the data have been analysed fitted and plotted by the software Origin® 8.0 Pro. All experiments have been carried out using quartz cuvettes of 1 cm<sup>2</sup> cross-sections purchased from Hellma Analytics.

### Lipophilicity and Solubility Calculations

Lipophilicity in terms of calculated logP (clogP) and solubility in terms of calculated logS (clogS) are determined at Virtual Computational Chemistry Laboratory server (<http://www.vcclab.org/lab/alogps>) [50]. Polar surface area is calculated with a 1.4 Å radius probe size.

### Molecular Docking

Molecular docking experiments have been performed using AutoDock Vina (Trott and Olson 2010) of The Scripps Research Institute [51] and the SwissDock server (<http://www.swissdock.ch>). AutoDock Vina and SwissDock uses different algorithms and scoring functions for docking calculations, thus, provides a consensus of docking output [52]. AutoDock Tools [53] have been used for the preparation of ligands and proteins for docking with Vina. BSA (PDB: 3 V03) [54] and HSA (PDB: 1E78) (Bhattacharya et al. 2000) [55] structural information have been obtained from Protein Data Bank (Berman et al. 2000) [56]. The three dimensional structure of KTHC-57 is drawn in Avogadro [57] and geometry optimized *in vacuo* using the steepest descent followed by conjugate gradient algorithms.

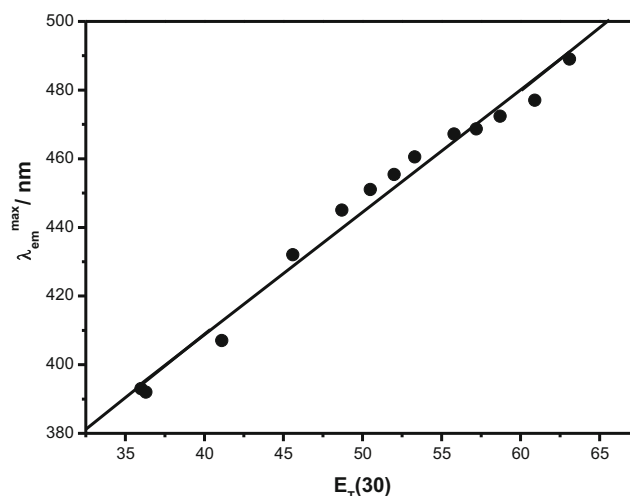


**Fig. 4** Variation of the emission maximum of KTHC-57 (Concentration of the compound is  $1 \times 10^{-6}$  M) with  $\epsilon_T(30)$  in dioxane–water mixtures

Molecular docking outputs are rendered in MGL Tools [53] and PyMOL Molecular Graphics System. Ligand interaction diagrams are generated in Schrodinger Maestro 9.8. UniProt residue numbering has been used for BSA and HSA sequences.

## Results and Discussion

### Fundamental Photophysical Possessions of KTHC-57 under Homogeneous and Micro-Heterogeneous Environments: A Brief Outline

Before moving into the details of confined photophysics of KTHC-57 within serum albumin confinement, it is relevant to cast light on its behaviour in homogeneous liquid so that we can appreciate the modulations to its photophysical properties in the confined state of serum albumins [49]. Enhancement of

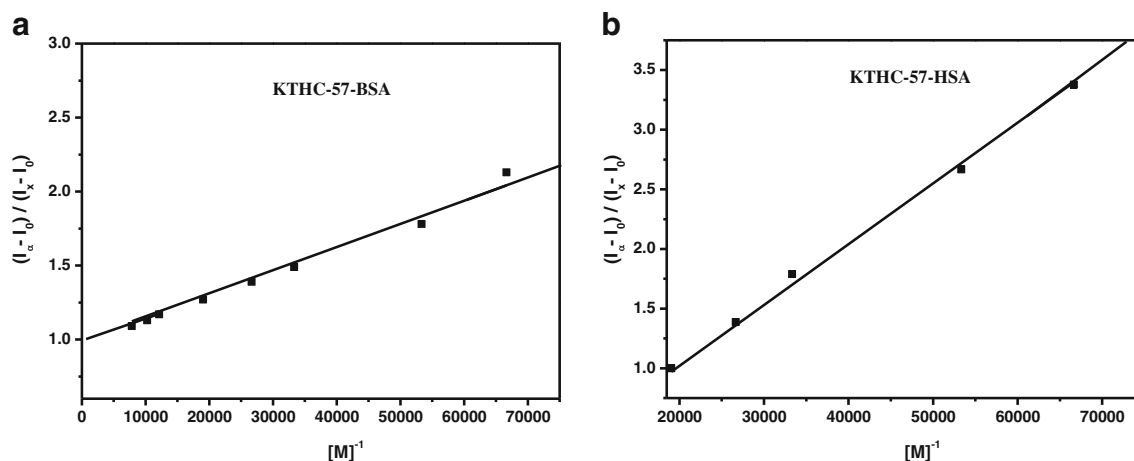


**Fig. 3** Benesi–Hildebrand plot of  $(I_x - I_0)/(I_x - I_0)$  vs.  $[M]^{-1}$  for complex formation between (a) KTHC-57-BSA and (b) KTHC-57-HSA. Concentration of the compound is  $1 \times 10^{-6}$  M. The linear regression indicates a 1:1 stoichiometry

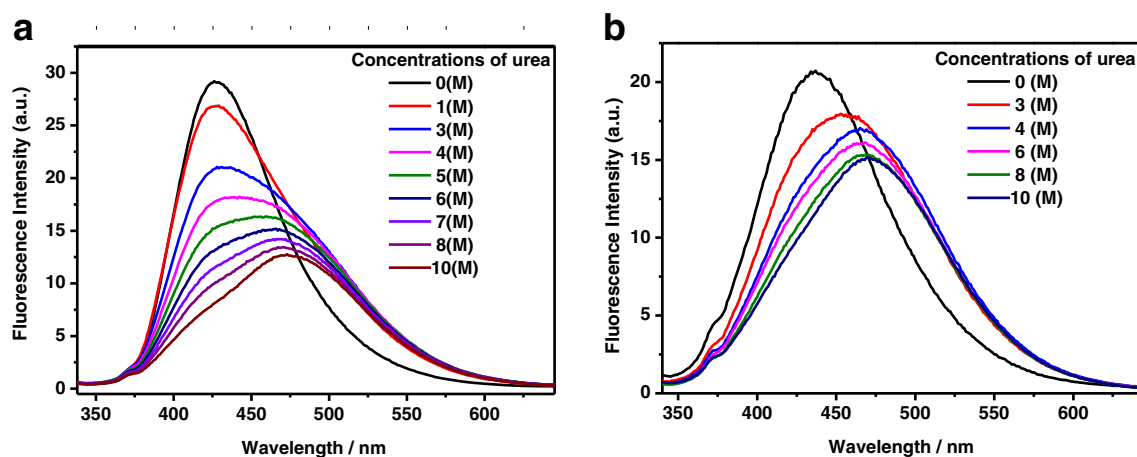


**Fig. 5** Fluorescence spectra of (a) BSA-bound and (b) HSA-bound KTHC-57 as a function of added urea. Concentration of the compound is  $1 \times 10^{-6}$  M

dipole moment of KTHC-57, a reporter of its immediate microenvironment, had been observed to be 11.72 D and 6.11 D in the case of protic and aprotic solvents respectively [49]. Excited state spectral features had been chiefly guided by two parameters namely, hydrogen bond donor acidity of the solvent and solvent dipolarity [49]. Even in the presence of different binary mixtures, appreciable changes in emission spectrum of KTHC-57 had been observed. Alterations in photophysical responses of KTHC-57 in different organized assemblies always had been noteworthy [49]. Considerable hypsochromic shift along with an enhancement of intensity had been the indication of entrapment of fluorophore in the hydrophobic regions of organised assemblies [49]. Monitoring the fluorosensing competence of KTHC-57 in various homogeneous, binary solvent mixtures and micro-heterogeneous environments interest has been paid to study its mode of interaction with albumin protein.

### Absorption and Fluorescence of KTHC-57 in Serum Albumin Environments

The fluorophore KTHC-57 shows a single absorption band at  $\sim 328$  nm for the  $\pi\pi^*$  transition of the aromatic chromophore in aqueous PBS. As seen in Fig. 1a and b, addition of proteins, both BSA and HSA to a solution of KTHC-57 results in a red shift with slight increase in absorbance of the absorption maxima from 328 nm in aqueous buffer to 330 nm in BSA and 333 nm in HSA on addition of 0.00100 (M) of protein in both the cases.

On the other side, remarkable modifications are observed in the emission profile of KTHC-57 with increasing concentrations of serum albumins (Fig. 2). Significant blue shift is observed ( $\sim 487$  nm in aqueous PBS to  $\sim 427$  nm and  $\sim 432$  nm in case of BSA and HSA respectively) along with marked intensity enhancement ( $\sim 3.7$  times in case of BSA and  $\sim 1.7$  times in case of HSA with respect to the fluorescence intensity observed in aqueous PBS). The shift in wavelength increases

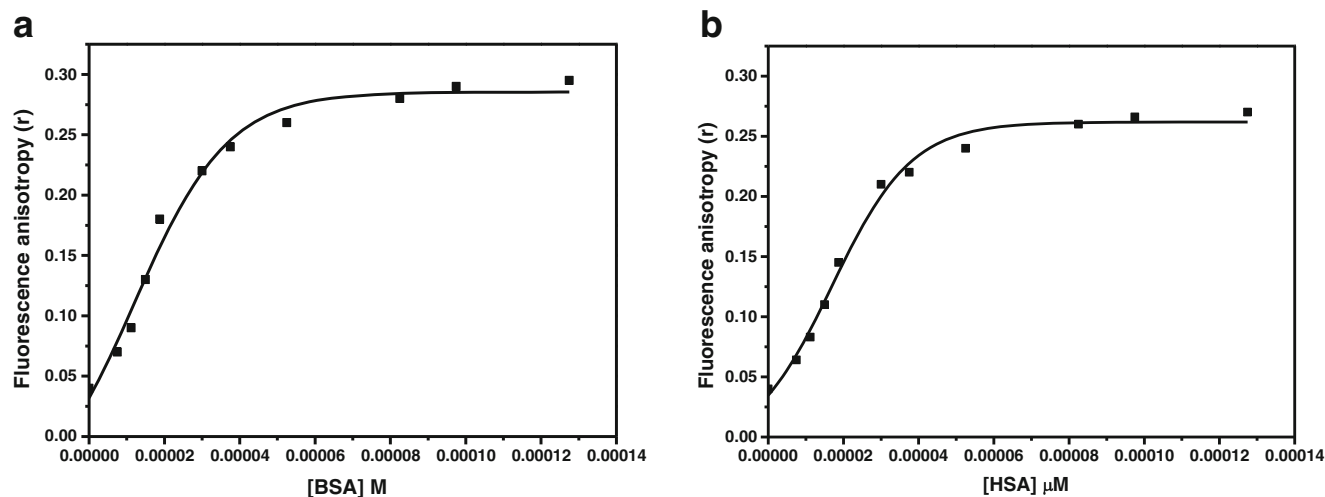


**Fig. 6** Variation of fluorescence anisotropy ( $r$ ) of KTHC-57 with increasing concentrations of (a) BSA and (b) HSA.  $\lambda_{em}$  is 427 nm for BSA and 432 nm for HSA. Concentration of the compound is  $1 \times 10^{-6}$  M



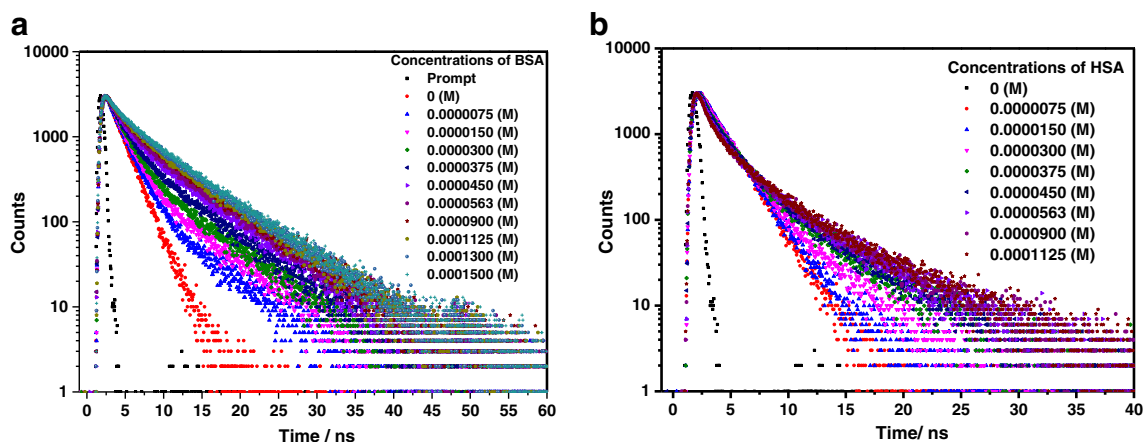


**Fig. 7** Fluorescence lifetime plots of KTHC-57 (excited using a 340 nm LED) in presence of BSA (a) and HSA (b). Concentration of the compound is  $1 \times 10^{-6}$  M

rapidly up to  $\sim 0.00001120$  M of BSA and  $\sim 0.00001125$  M of HSA concentration and then arrives at a flat region. Significant hypsochromic shift of emission maxima ( $\sim 60$  nm in case of BSA and  $\sim 55$  nm in case of HSA) with increasing concentration of protein advocates that KTHC-57 gets entrapped in the hydrophobic pockets i.e., in the less polar part of the protein molecules. Nevertheless, the hypsochromic shift on the emission profile of KTHC-57 with increasing concentrations of serum albumins should not be mistaken for the slight bathochromic shift observed in the case of absorption spectral profile as it is probably due to the enormously differential natures of the potential energy surfaces of the ground and excited states [58].

### KTHC-57 – Serum Albumin Binding

Changes in the spectral features with addition of proteins are indicative of interaction between KTHC-57 and protein. A quantitative estimate or the extent of binding of KTHC-57 to the hydrophobic cavity of proteins is determined using the re-ordered Benesi–Hildebrand relation [58]:

$$(I_{\infty} - I_0) / (I_x - I_0) = 1 + (K[M])^{-1} \quad (3)$$

**Table 1** Fluorescence lifetime of KTHC-57 with increasing concentration of HSA

HSA (concentration)	$(a_1)/(a_2)$	$\tau_1 / \tau_2$ (ns)	$\chi^2$	$\tau_{av}$ (ns)
0 M	(1)/(0)	1.92	0.99	1.92
0.0000075 M	(0.67)/(0.33)	1.72/2.55	1.03	1.99
0.0000150 M	(0.65)/(0.35)	1.60/3.61	1.09	2.30
0.0000300 M	(0.60)/(0.40)	1.40/4.52	1.19	2.65
0.0000375 M	(0.53)/(0.47)	1.20/4.55	1.21	2.77
0.0000450 M	(0.46)/(0.54)	0.94/4.65	1.18	2.94
0.0000563 M	(0.44)/(0.56)	0.72/4.91	1.02	3.07
0.0001125 M	(0.40)/(0.60)	0.68/5.01	1.17	3.28

Where,  $I_0$ ,  $I_x$  and  $I_{\infty}$  are the fluorescence intensities of KTHC-57 considered in the absence of protein at an intermediate protein concentration and at a concentration for complete interaction, respectively;  $K$  being the binding constant and  $[M]$  is the free protein concentration. A plot of  $(I_{\infty} - I_0) / (I_x - I_0)$  against  $[M]^{-1}$  shows linear variation justifying the validity of the Benesi–Hildebrand equation for the present case and therefore, settles 1:1 stoichiometry for the probe: protein complex (Fig. 3).

The values of  $K$  thus obtained at 298 K are  $64,009 \text{ M}^{-1}$  for BSA ( $\Delta G = -RT \ln K = -27.42 \text{ kJ mol}^{-1}$ ) and  $19,610 \text{ M}^{-1}$  for HSA ( $\Delta G = -RT \ln K = -24.49 \text{ kJ mol}^{-1}$ ). Free energy change indicates spontaneity of complexation process for both cases. The binding constant values indicate the relative stabilities of the dye–protein complexes and it can be deduced that the dye binds in a stronger way to BSA than HSA.

### Polarity of the Microenvironment Surrounding KTHC-57 in Serum Albumin Environments

It has been a couple of decades, a unique role has been played by various types of fluorophores (as the situation claims) in the determination of the microscopic polarity of the biological environments. Here, in this communication we have made an attempt

**Table 2** Fluorescence lifetime of KTHC-57 with increasing concentration of BSA

BSA (concentration)	$(a_1)/(a_2)$	$\tau_1 / \tau_2$ (ns)	$\chi^2$	$\tau_{av}$
0 M	(1)/(0)	1.92	0.99	1.92
0.0000075 M	(0.81)/(0.19)	1.92/6.82	1.01	2.851
0.0000150 M	(0.71)/(0.29)	1.91/6.83	1.02	3.3368
0.0000300 M	(0.61)/(0.39)	1.93/6.97	1.01	3.8956
0.0000375 M	(0.48)/(0.52)	1.88/7.04	1.05	4.5632
0.0000450 M	(0.32)/(0.68)	1.97/7.09	1.07	5.4516
0.0000563 M	(0.25)/(0.75)	1.93/7.11	1.00	5.815
0.0001125 M	(0.16)/(0.84)	1.73/7.15	1.09	6.2828

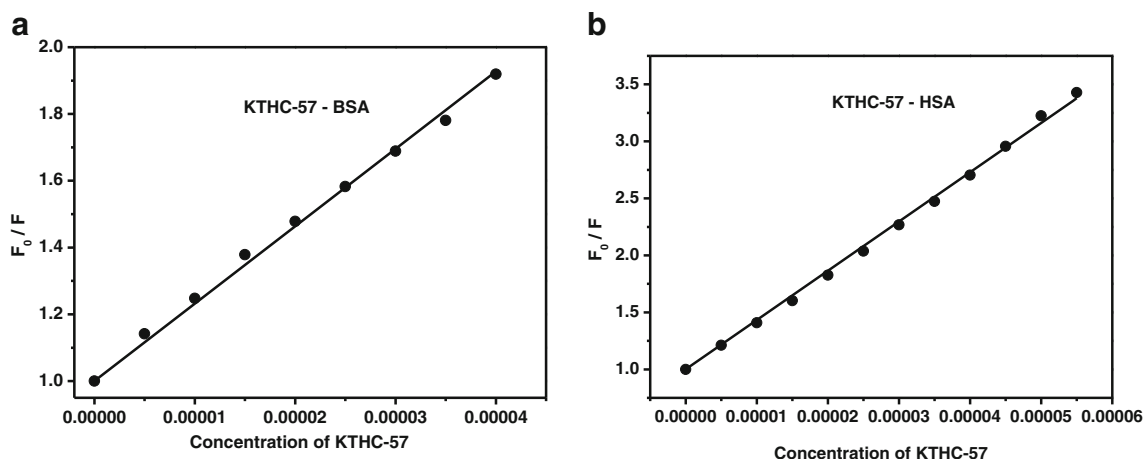


**Fig. 8** Stern-Volmer plot for the quenching of (a) BSA and (b) HSA fluorescence with KTHC-57 with the data obtained from Fig. 9(a) and (b) respectively

regarding the estimation of micropolarity of the proteinous environments around the fluorophore, considering the fact that no other research group has ever thought of using keto-tetrahydrocarbazole based fluorophores for the determination of micropolarity in proteins.

Many examples can be cited where the local polarity of proteins has been estimated by comparing the emission features of the fluorophore in that proteinous environment with those spectra obtained from the same molecule in solvents of known polarities [58–60]. It is worthy to mention that polarity of a homogeneous environment is not exactly the same as the polarity in a protein medium owing to a different type of solvent relaxation. However, to make a qualitative assessment regarding micropolarities in BSA and HSA environment, the fluorescence behaviour of KTHC-57 within this protein environment has been compared to that in water-dioxane mixture of varying composition. Figure 4 indicates that micropolarities of BSA and HSA are determined to be 45.24 and 46.5 respectively on the  $E_T(30)$  scale which is considerably low compared to the  $E_T(30)$  of bulk water (63.145) and hence accounts for the blue shift of the emission band of KTHC-57.

### Effect of Urea on Serum Albumin Bound KTHC-57

Perceiving the binding interaction between the KTHC-57 and BSA / HSA, we have attempted to understand the denaturing effect of the protein on its binding activity and on the overall photophysics of KTHC-57. Monitoring the unfolding process of serum albumins on increasing concentration of urea has been well studied and literature report reveals that on increasing the concentrations of urea denaturation of serum albumins takes place at a single, two-state transition through intermediate state at 4–6 mol / L urea. Using the steady-state fluorescence measurements, in the present report we have studied urea-induced modification of the protein bound drug (KTHC-57). On steady addition of the urea to the protein-bound KTHC-57, the emission profile (Fig. 5) undergoes a significant bathochromic shift and lowering of fluorescence intensity is observed, opposite to that observed in Fig. 2. Water molecules adjacent to the fluorophore KTHC-57 within protein environment are displaced by urea and the destabilisation thus caused leads to the desolvation of the guest molecule.

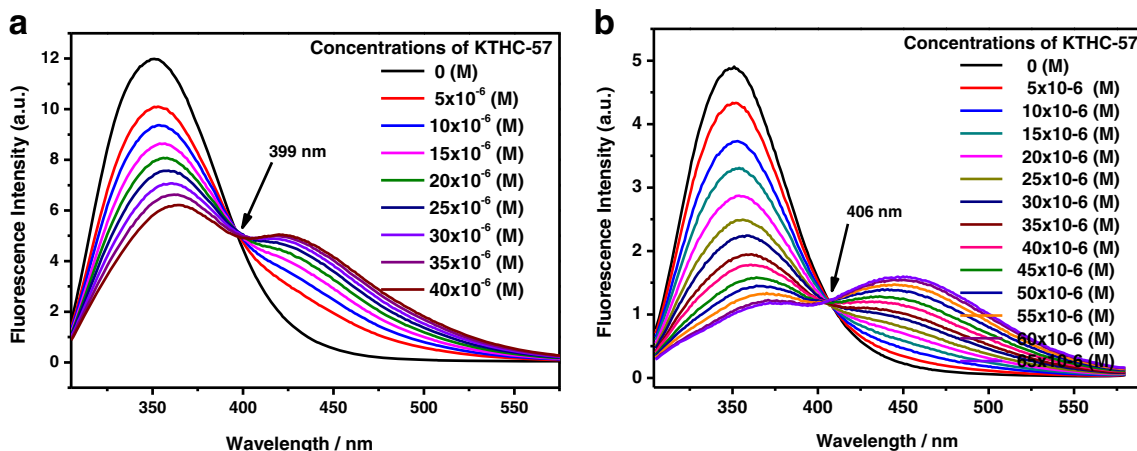


**Fig. 9** Fluorescence spectra of (a) BSA and (b) HSA as a function of KTHC-57 concentrations ( $\lambda_{exc} = 280$  nm) in aqueous PBS buffer solution

**Table 3** Stern-Volmer constants for the quenching of the fluorescence of HSA and BSA with KTHC-57

Protein	$K_{SV}$ in $M^{-1}$
HSA	43,246.89
BSA	23,184.03

### Steady State Fluorescence Anisotropy Study of KTHC-57 in Serum Albumin Environments

Fluorescence anisotropy is a long recognised delicate tool towards the sensing of degree of restrictions imparted by the micro-environments of serum albumins [58, 61, 62]. This technique is useful to assess the probable location of the fluorophore in the confined medium. Nothing can be better to affirm our interpretations if the conclusions derived from the steady-state fluorescence measurements are best complemented with the anisotropy values.

Fluorescence anisotropy of KTHC-57 increases (Fig. 6) as the concentration of BSA and HSA increases ( $r = 0.29$  in case of BSA and  $r = 0.26$  in case of HSA). Gradual increase in fluorescence anisotropy with increase in concentrations of protein reveals that the rotational diffusion of KTHC-57 is significantly constrained in the proteinous medium. A fairly higher anisotropy value is obtained from BSA than HSA and it points to a comparatively better binding interaction between KTHC-57 and BSA, harmonizing the values of complexation constant ( $K$ ) and free energy change ( $\Delta G$ ).

### Fluorescence Lifetime of KTHC-57 in Serum Albumin Environments

Fluorescence lifetime experiments are usually recognised as a sensitive indicator to interrogate the excited state affairs of a fluorophore. This study significantly helps us to understand

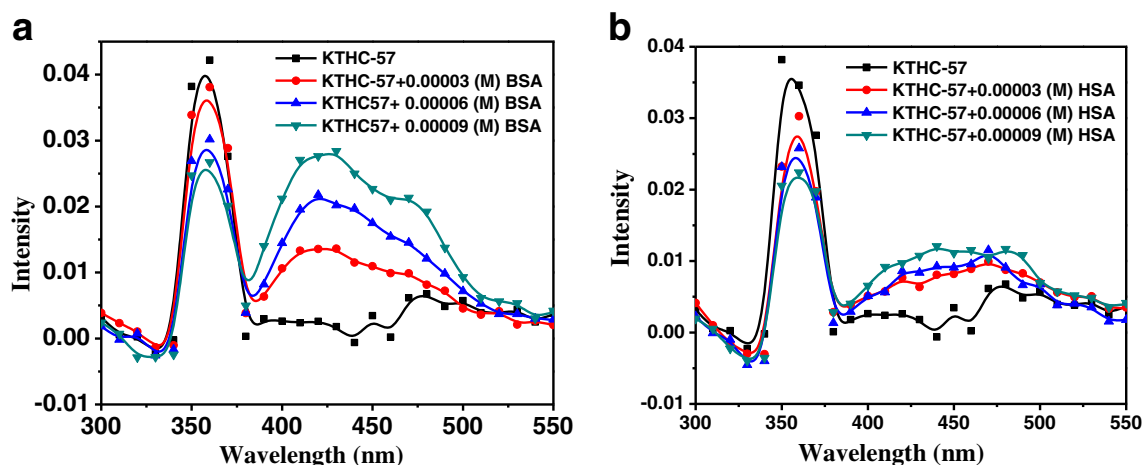
**Table 4** Changes in lifetime at 357 nm and at 430 nm in presence of HSA

Decay @	357 nm	430 nm
KTHC-57 only	$2.05 \pm 0.003 \mu S$	$1.72 \pm 0.005 \mu S$
KTHC-57 + 50 ul HSA	$1.89 \pm 0.001 \mu S$	$1.84 \pm 0.001 \mu S$
KTHC-57 + 100ul HSA	$1.87 \pm 0.002 \mu S$	$1.89 \pm 0.002 \mu S$
KTHC-57 + 200ul HSA	$1.85 \pm 0.004 \mu S$	$2.01 \pm 0.004 \mu S$

the differential degrees of solvent relaxation around a fluorophore in the excited state. Presence of more than one chemical entity in a solution is also indicated by Fluorescence lifetime experiments.

In aqueous PBS, KTHC-57 displays a single-exponential decay with a lifetime of around 1.92 ns whereas, in the serum albumin environments bi-exponential decay of KTHC-57 is observed with a longer lifetime component along with the original one observed in the aqueous PBS medium. Typical decay profiles of KTHC-57 in the two protein environments are shown in Fig. 7 and the deconvoluted data are represented in Tables 1 and 2.

Here, for a similar increase in concentration of both the proteins, average lifetime ( $\tau_{av}$ ) of KTHC-57 increases to a greater extent in BSA (~1.92 ns to ~6.28 ns) than in HSA (~1.92 ns to ~3.28 ns). This indicates that motional restriction is comparatively higher in case of BSA than in HSA. If we go through the Tables 1 and 2, it is evident that the comparatively shorter lifetime component is due to the free probe in aqueous PBS and the longer lifetime component can be assigned to the fluorescence coming from the probe–protein complex. Considerably higher lifetime value of the BSA- bound KTHC-57 is observed than the HSA- bound KTHC-57 suggests lower polarity in BSA micro-environment than in HSA environment. This observation further advocates the fact that, KTHC-57 is buried deeper in BSA than in HSA.

**Fig. 10** Transient triplet-triplet absorption spectra of KTHC-57 ( $1 \times 10^{-6}$  M) in aqueous PBS with (a) BSA and (b) HSA  $1 \mu s$  after laser flash



**Table 5** Changes in lifetime at 357 nm and at 430 nm in presence of BSA

Decay @	360 nm	430 nm
KTHC-57 only	2.1 ± .001 μS	1.72 ± 0.004 μS
KTHC-57 + 50 ul BSA	1.86 ± .006 μS	1.86 ± 0.002 μS
KTHC-57 + 100ul BSA	1.83 ± 0.005 μS	1.88 ± 0.003 μS
KTHC-57 + 200ul BSA	1.82 ± 0.002 μS	2.2 ± 0.003 μS

### Perturbation in the Fluorescence Emission of Serum Albumins on Addition of KTHC-57:

The attenuation of fluorescence intensity,  $F$  of the proteins on interaction with KTHC-57 is expressed with the following Stern-Volmer equation [63]:

$$\frac{F_0}{F} = 1 + K_{SV}[Q] \quad (4)$$

Where,  $K_{SV}$  is the Stern-Volmer quenching constant. Figure 8 represents the Stern-Volmer plot for the quenching of the fluorescence of BSA and HSA with KTHC-57 (data obtained from Fig. 9). Table 3 lists the corresponding Stern-Volmer constants. Linear Stern-Volmer plots may either indicate the existence of just a binding site for KTHC-57 in the proximity of the tryptophan, or the existence of more than one site spatially arranged so that they are equally accessible to KTHC-57 [58].

### Laser Flash Photolysis

Laser flash photolysis experiment has been carried out to investigate the transient state behaviour of proposed KTHC-57-BSA/HSA complex. The transient absorption spectra of KTHC-57 (Fig. 10) with increasing concentration of BSA and HSA indicate that only KTHC-57 (i.e., absence of albumin proteins) absorbs at 357 nm and 430 nm. With the gradual addition of BSA

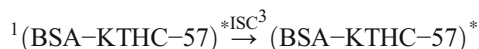
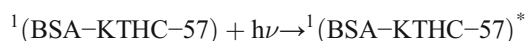
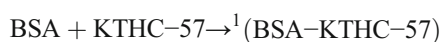
**Table 6** Molecular properties of KTHC-57.

<sup>a</sup>The data represents mean ± SD

logP <sup>a</sup>	2.32 ± 0.54
logS	−3.07
Polar surface area (Å <sup>2</sup> )	51.32
Lipinski's rule of five	Yes

and HSA, the peak intensity at 357 nm decreases with simultaneous increase at 430 nm. Moreover, an isosbestic point is observed at 378 nm which supports the formation of KTHC-57-BSA and KTHC-57-HSA complex which absorbs at 430 nm.

The probable cause of complex formation is the presence of tyrosine and positively charged amino acids arginine/lysine in both the serum albumins. KTHC-57 has extensive pi-electron cloud indicating possible pi-stacking and pi-cation interactions with the above mentioned residues.



The triplet life time analysis (Tables 4 and 5) indicates that KTHC-57 forms more stable complex with BSA than HSA as shown in the decay profile also (Fig. 11). This phenomenon may happen due to the different proximity effect of pi-electron cloud of KTHC-57 within the protein environment which is further confirmed by theoretical modelling.

### Molecular Docking Analysis

#### Drug like Properties of KTHC-57

The molecular properties of KTHC-57, such as clogP, clogS, polar surface area etc. [64] are listed in Table 6. The clogP value of a compound is the logarithm of its partition coefficient

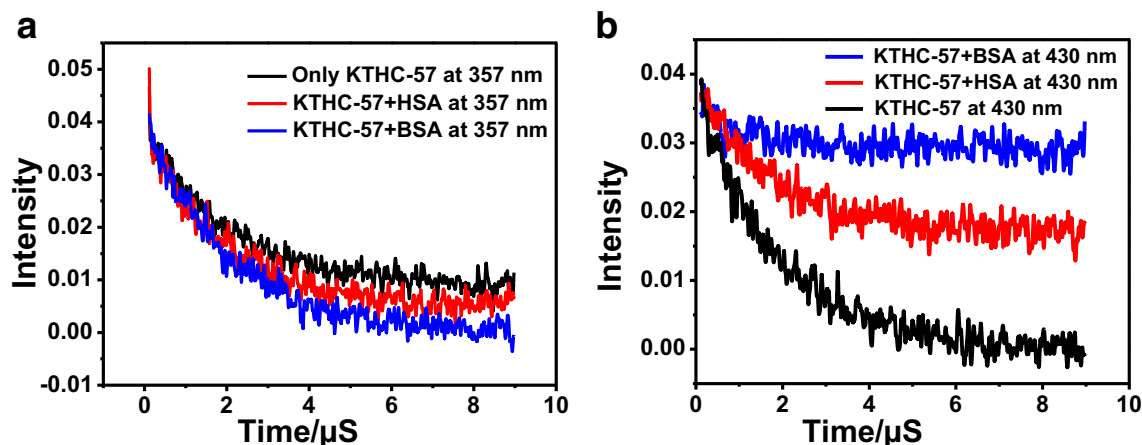


**Fig. 11** Decay profiles of KTHC-57 with 0.00006 (M) of BSA and HSA at (a) 357 nm and (b) 430 nm after the laser flash at 355 nm

**Table 7** Theoretical binding free energies as obtained by molecular docking experiments using two different algorithms, AutoDock Vina and SwissDock

Complexes	AutoDock Vina (kJ mol <sup>-1</sup> )	SwissDock (kJ mol <sup>-1</sup> )
BSA-KTHC57	-33.96	-29.58
HSA-KTHC57	-33.05	-29.29

between n-octanol and water. It is a well established measure of the compound's lipophilicity which influences its behaviour in a range of biological processes such as solubility, membrane permeability, lack of selectivity and non-specific toxicity [65]. It has been shown for compounds to have a reasonable probability of being well absorbed, their logP value must not be greater than 5.0 [66]. Besides, the aqueous solubility of a compound is also defined by logS which significantly affects its absorption and distribution characteristics. Typically, a low solubility goes along with a bad absorption. Most of the drugs in the market have an estimated logS value of about -4. Table 6 lists the polar surface area of the compound as well which should be less than 140 Å<sup>2</sup> for a drug molecule [66]. Apart from lipophilicity/solubility and the polar surface area, the molecular weight and the number of hydrogen bond acceptors/donors in KTHC-57 also follow the Lipinski's rule of five [66] to be candidate drug molecules.

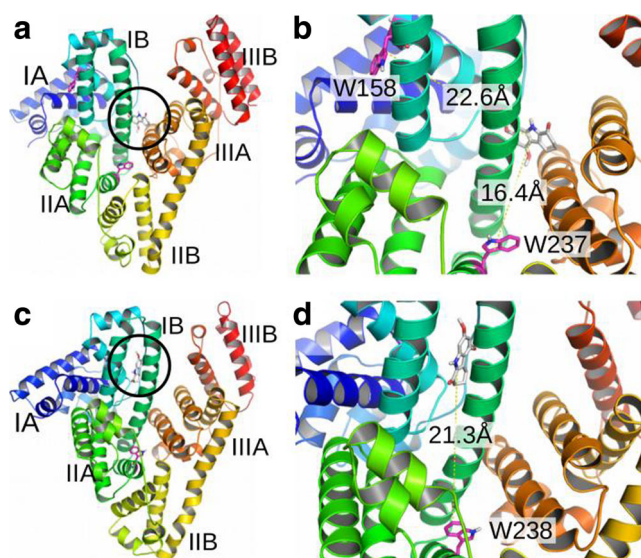


**Fig. 12** Interaction of KTHC-57 with serum albumins as obtained from molecular docking experiments. **a** Best binding conformation of KTHC-57 with BSA. Binding site is marked with a circle. **b** Close up view of KTHC-57 binding with BSA. Distances from the two tryptophan residues are shown. **c** Best binding conformations of KTHC-57 with HSA. Binding site is marked with a circle. **d** Close up view of KTHC-57 in the binding site of HSA. Distance from tryptophan 238 is shown. AutoDock Vina generated complexes are depicted here. Proteins are shown in ribbon diagram; tryptophans and the ligands are shown in stick model. The three domains of serum albumin are marked with I–III. Standard colour representation is used to denote the elements, H, N and O in the ligand

### Molecular Modeling

In silico molecular docking calculation shows that the interactions of KTHC-57 with serum albumins are thermodynamically favourable (Table 7). The binding free energies computed by AutoDock Vina and SwissDock are close to that of the experimentally obtained values. Molecular docking also provides the insight into the most favourable binding site for these compounds on the serum albumins. The lowest energy complexes obtained by two different algorithms consistently have shown that the binding sites for KTHC-57 lay in the groove between domain I and domain III of BSA, whereas it is within the domain I in case of HSA (Fig. 12). Serum albumin with its

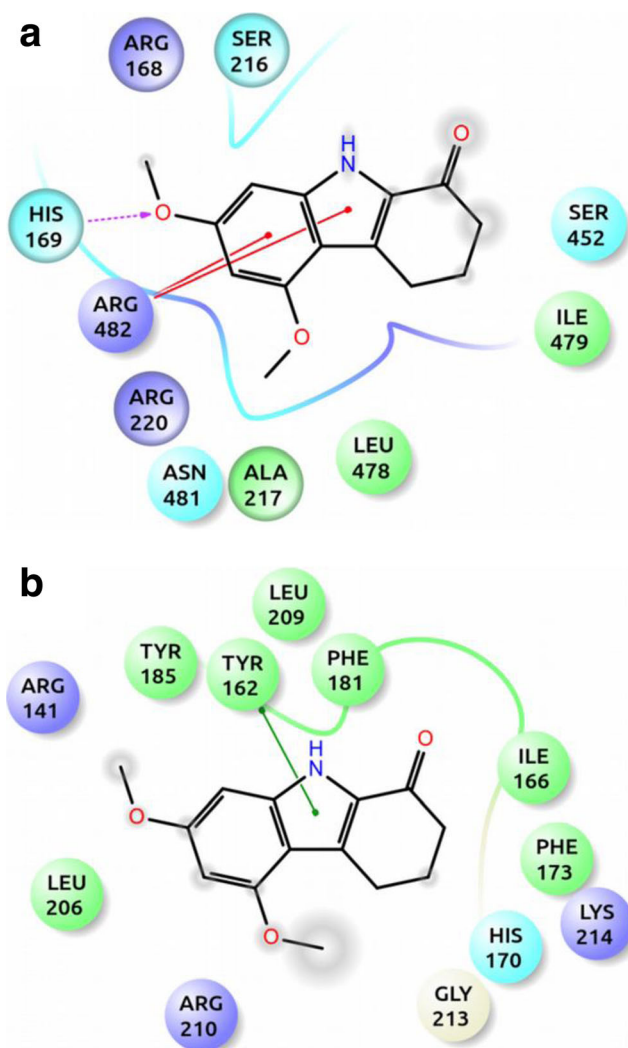


**Fig. 13** Detailed interaction diagram of KTHC-57 with serum albumins as obtained by molecular docking experiments. **a** Interacting residues of BSA and the types of interactions with KTHC-57. Histidine 169 forms a hydrogen bond with KTHC-57 whereas arginine 482 forms pi-cation interaction. **b** Interacting residues of HSA and the types of interactions with KTHC-57. pi-stacking occurs with tyrosine 162. Green indicates hydrophobic residues; polar residues are colored in cyan. Positively charged residues are shown in purple

many hydrophobic binding pockets acts like a universal receptor for almost all drug molecules. Binding to serum albumin is generally non-specific in nature and driven by mainly hydrophobic interactions [52].

Detailed interaction diagrams of the protein–ligand complexes showing the interacting residues and the types of interactions obtained by molecular modeling are given in Fig. 13. We have found that binding site for KTHC-57 lines in the groove between domain I and III of BSA and in domain I of HSA (Fig. 12). His169 of BSA has been found to form a hydrogen bond with KTHC-57 whereas Arg482 forms pi-cation interaction with the ligand. Other important interacting residues of BSA are Arg168, Ser216, Ala217, Arg220, Ser452, Leu478, Ile479 and Asn481. In case of HSA, KTHC-57 forms pi-stacking interaction with Tyr162. Other hydrophobic amino acids surrounding KTHC-57 in the groove of HSA are Ile166, Phe173, Phe181, Tyr185, Leu206 and Leu209. Polar amino acid His170 and the positively charged Arg141, Arg210 and Lys214 are also important for the binding of KTHC-57 with HSA (Fig. 13).

## Summary and Conclusion

The present work reports a study of the interaction of a recently developed keto-tetrahydrocarbazole based fluorosensor, KTHC-57, with BSA and HSA proteins. Excited state photophysics of KTHC-57 gets remarkably modified on addition of albumin proteins compared to that observed in aqueous phase. This has been exploited to explore the binding efficiency, the nature of the microenvironment around the fluorophore and the micropolarity at the binding site. Above studies indicate that KTHC-57 binds with both BSA and HSA; the binding is, however, stronger with the former. In this work, the denaturing action of urea toward the albumin proteins is demonstrated, throwing some light on the probable binding location of the drug in the proteinoous environment. We have found that binding site for KTHC-57 lines in the groove between domain I and III of BSA and in domain I of HSA. KTHC-57 is thus proved to a potential indicator to follow different aspects of the bio and organized assemblies. Last but not the least, based on a comparative platform between two albumin proteins BSA and HSA, our fluorophore of interest KTHC-57 interacts and binds to a greater extent with BSA than it does with HSA.

**Acknowledgements** This work has been funded by Chemical and Biophysical Approaches for Understanding of Natural Processes (CBAUNP) project, SINP of the Department of Atomic Energy (DAE), Government of India. Thanks to CSIR, New Delhi for providing financial help in the form of fellowships. Special thanks to Mr. Amartya Krishna Mitra for being a constant source of inspiration. We also want to thank Mrs. Sayantani Mitra for her sincere support in perusing the paper and making suitable modifications in language.

## References

- Brown JR, Rosenoer VM, Oratz M, Rothschild MA (1977) Albumin structure, function and uses. Pergamon Press, Oxford
- Sharma RN, Pancholi SS (2014) *Int J Pharm Pharm Sci* 6:726
- Carter DC, Ho JX (1994) *Adv Protein Chem* 45:153
- Bojesen E, Bojesen IN (1996) *J Phys Chem* 100:17981
- Karachentsev AN, Melchenko IA (1997) *Eksp Klin Farmakol* 60:68
- Ali MS, Al Lohedan HA (2014) *J Mol Liq* 197:124
- Kandagal PB, Ashoka S, Seetharamappa J, Shaikh SMT, Jadegoud Y, Ijare OB (2006) *J Pharm Biomed Anal* 41:393
- Ali MS, Al Lohedan HA (2013) *Mol Biol Rep* 40:6081
- Sengupta B, Sengupta PK (2002) *Biochem Biophys Res Commun* 299:400
- Yang GD, Li C, Zeng AG, Zhao Y, Yang R, Brian XL (2013) *J Pharm Anal* 3:200
- Klopfenstein WE (1969) *Biochim Biophys Acta* 187:272
- Khan SN, Islam B, Yennamalli R, Sultan A, Subbarao N, Khan AU (2008) *Eur J Pharm Sci* 35:371
- Mathew MK, Balaran P (1980) *FEBS Lett* 115:91
- Makino S, Reynolds JA, Tanford C (1973) *J Biol Chem* 248:4926
- Lin H, Lan J, Guan M, Sheng F, Zhang H (2009) *Spectrochim Acta A Mol Biomol Spectrosc* 73:936
- Bal W, Christodoulou J, Sadler PJ, Tucker A (1998) *J Inorg Biochem* 70:33
- Khan AB, Khan JM, Ali MS, Khan RH, Din KU (2012) *Spectrochim Acta A Mol Biomol Spectrosc* 97:119
- Gelamo EL, Tabak M (2000) *Spectrochim Acta A* 56:2255
- Gelamo EL, Silva CH, Imasato H, Tabak M (2002) *Biochim Biophys Acta* 84:1594
- Yang L, Lv J, Wang X, Zhang J, Qi L, Zhang T, Zhang Z, Zhang L (2015) *J Mol Recognit* 28:459
- Rawel HM, Meidtner K, Kroll J (2005) *J Agric Food Chem* 53:4228
- Hu YJ, Liu Y, Zhang LX, Zhao RM, Qu SS (2005) *J Mol Struct* 750:174
- Jayabharathi J, Thanikachalam V, Perumal MV (2012) *J Lumin* 132:707
- Shen L, Yang Z, Tang R (2012) *Spectrochim Acta A Mol Biomol Spectrosc* 98:170
- Zhu Y, Zhang R, Wang Y, Ma J, Li K, Li Z (2014) *J Photochem Photobiol B Biol* 140:381
- Shahabadi N, Hadidi S, Feizi F (2015) *Spectrochim Acta A Mol Biomol Spectrosc* 138:169
- Dufour C, Dangles O (2005, 1721) *Biochim Biophys Acta Gen Subj*:164
- Sijmons PC, Dekker BMM, Schrammeijer B, Verwoerd TC, Van den Elzen PJM, Hoekema A (1990) *BioTechniques* 8:217
- Moriyama Y, Ohta D, Hadiya K, Mitsui Y, Takeda K (1996) *J Protein Chem* 15:265
- Mikusinska-Planner A, Surma M (2000) *Spectrochim Acta A* 56:1835
- Kumar CV, Buranaprapuk A (1997) *Angew Chem Int Ed England* 36:2085
- Hu YJ, Liu Y, Xiao XH (2009) *Biomacromolecules* 10:517
- Lhiaubet-Vallet V, Sarabia Z, Bosca F, Miranda MA (2004) *J Am Chem Soc* 126:9538
- He XM, Carter DC (1992) *Nature* 358:209
- Jimenez MC, Miranda MA, Vaya I (2005) *J Am Chem Soc* 127:10134
- Szacilowski K, Macyk W, Drzewiecka-Matuszek A, Brindell M, Stochel G (2005) *Chem Rev* 105:2647

37. Pandey RK, Constantine S, Tsuchida T, Zheng G, Medforth CJ, Aoudia M, Kozyrev AN, Rogers MAJ, Kato H, Smith KM, Dougherty TJ (1997) *J Med Chem* 40:2770
38. Patrice T (2004) Photodynamic therapy, Royal Society of Chemistry (GB)
39. Peters T (1985) Serum albumin, advances in protein chemistry, vol 37. Academic Press, New York
40. Kar C, Ojha B, Das G (2013) *J Lumin* 28:339
41. Helms MK, Peterson CE, Bhagavan NV, Jameson DM (1997) *FEBS Lett* 408:67
42. Pavldridge W, Am M (1987) *J Physiol* 252:157
43. Gonzalez-Jimenez J, Cortijo M (2002) *J Protein Chem* 21:75
44. Sulkowska A, Bojko B, Rownicka J, Pentak D, Sulkowska W (2003) *J Mol Struct* 651:237
45. Tayyab S, Sharma N, Khan MM (2000) *Biochem Biophys Res Commun* 277:83
46. Ahmad B, Khan MKA, Haq SK, Khan RH (2004) *Biochem Biophys Res Commun* 314:166
47. Cohen BE, Pralle A, Yao XJ, Swaminath G, Gandhi CS, Jan YN, Kobilka BK, Isacoff EY, Jan LY (2005) *Proc Natl Acad Sci U S A* 102:965
48. Banerjee M, Pal U, Subudhhi A, Chakrabarti A, Basu S (2012) *J Photochem Photobiol B Biol* 108:23
49. Mitra AK, Ghosh S, Sau A, Saha C, Basu S (2015) *J Lumin* 167:233
50. Tetko IV, Gasteiger J, Todeschini R, Mauri A, Livingstone D, Ertl P, Palyulin VA, Radchenko EV, Zefirov NS, Makarenko AS (2005) *J Comput Aided Mol Des* 19:453
51. Trott O, Olson AJ (2010) *J Comput Chem* 31:455
52. Pal U, Pramanik SK, Bhattacharya B, Banerji B, Maiti NC (2015) *SpringerPlus* 4:548
53. Morris GM, Huey R, Lindstrom W, Sanner MF, Belew RK, Goodsell DS, Olson AJ (2009) *J Comput Chem* 30:2785
54. Majorek KA, Porebski PJ, Dayal A, Zimmerman MD, Jablonska K, Stewart AJ, Chruszcz M, Minor W (2012) Structural and immunologic characterization of bovine, horse, and rabbit serum albumins. *Mol Immunol* 52:174
55. Bhattacharya AA, Curry S, Franks NP (2000) *J Biol Chem* 275:38731
56. Berman HM, Westbrook J, Feng Z, Gilliland G, Bhat TN, Weissig H, Shindyalov IN, Bourne PE (2000) *Nucleic Acids Res* 28:235
57. Hanwell MD, Curtis DE, Lonie DC, Vandermeersch T, Zurek E, Hutchison GR (2012) *J Cheminformatics* 4:17
58. Lakowicz JR (1999) Principles of fluorescence spectroscopy; Plenum: New York
59. Krishnakumar SS, Panda D (2002) *Biochemistry* 41:7443
60. Macgregor RB, Weber G (1986) *Nature* 319:70
61. Mallick A, Haldar B, Maiti S, Bera SC, Chattopadhyay N (2005) *J Phys Chem B* 109:14675
62. Chakrabarty A, Mallick A, Haldar B, Das P, Chattopadhyay N (2007) *Biomacromolecules* 8:920
63. Stern O, Volmer M (1919) Über die Abklingungszeit der Fluoreszenz. *Phys Z* 20:183
64. Bickerton GR, Paolini GV, Besnard J, Muresan S, Hopkins AL (2012) *Nat Chem* 4:90
65. Alam A, Pal C, Goyal M, Kundu MK, Kumar R, Iqbal MS, Dey S, Bindu S, Sarkar S, Pal U (2011) *Bioorg Med Chem* 19:7365
66. Lipinski CA, Lombardo F, Dominy BW, Feeney PJ (1997) *Adv Drug Deliv Rev* 23:3